

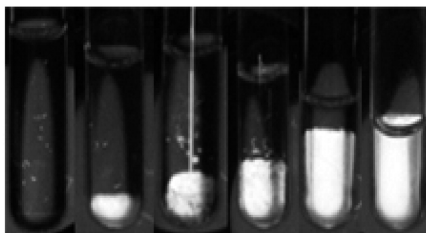
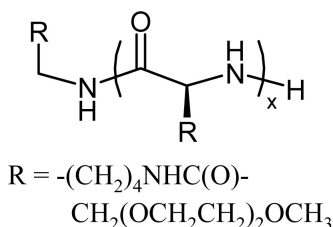
Article

Aqueous Cholesteric Liquid Crystals Using Uncharged Rodlike Polypeptides

Enrico G. Bellomo, Patrick Davidson, Marianne Impror-Clerc, and Timothy J. Deming

J. Am. Chem. Soc., **2004**, 126 (29), 9101-9105 • DOI: 10.1021/ja047932d • Publication Date (Web): 02 July 2004

Downloaded from <http://pubs.acs.org> on March 31, 2009



More About This Article

Additional resources and features associated with this article are available within the HTML version:

- Supporting Information
- Links to the 3 articles that cite this article, as of the time of this article download
- Access to high resolution figures
- Links to articles and content related to this article
- Copyright permission to reproduce figures and/or text from this article

[View the Full Text HTML](#)

Aqueous Cholesteric Liquid Crystals Using Uncharged Rodlike Polypeptides

Enrico G. Bellomo,[†] Patrick Davidson,[‡] Marianne Impéror-Clerc,[‡] and Timothy J. Deming^{*†}

Contribution from the Departments of Materials and Chemistry, Materials Research Laboratory, University of California, Santa Barbara, California 93106, and Laboratoire de Physique des Solides, UMR 8502 CNRS, Bât. 510, Université d'Orsay, F-91405 Orsay, France

Received April 9, 2004; E-mail: tdeming@mrl.ucsb.edu

Abstract: The aqueous, lyotropic liquid-crystalline phase behavior of the α -helical polypeptide, poly(N_ϵ -2-[2-(2-methoxyethoxy)ethoxy]acetyl-lysine) (**1**), has been studied using optical microscopy and X-ray scattering. Solutions of optically pure **1** were found to form cholesteric liquid crystals at volume fractions that decreased with increasing average chain length. At very high volume fractions, the formation of a hexagonal mesophase was observed. The pitch of the cholesteric phase could be varied by a mixture of enantiomeric samples **L-1** and **D-1**, where the pitch increased as the mixture approached equimolar. The cholesteric phases could be untwisted, using either magnetic field or shear flow, into nematic phases, which relaxed into cholesterics upon removal of field or shear. We have found that the phase diagram of **1** in aqueous solution parallels that of poly(γ -benzyl glutamate) in organic solvents, thus providing a useful system for liquid-crystal applications requiring water as solvent.

Introduction

Aqueous, lyotropic liquid crystals have great potential for a wide range of applications. These include use as templates for biomimetic inorganic materials synthesis¹ and as electric-field responsive materials in actuators and devices.² Furthermore, cholesteric aqueous liquid crystals would be valuable as chiral NMR solvents for enantiomer resolution,³ and as a chiral medium for asymmetric transformations.⁴ In the area of polypeptide liquid crystals, poly(γ -benzyl-L-glutamate) (PBLG) is perhaps the best studied example.⁵ This rodlike, α -helical polymer forms cholesteric liquid crystals in a number of organic solvents at concentrations above ca. 20 wt %, depending on chain length and temperature.⁶ Unfortunately, there is no aqueous phase polypeptide analogue of PBLG, even though the organic system has been known for over 40 years. A good reason for this has been the lack of a water-soluble, α -helical homopolypeptide.

The repulsion of abundant-like charges on most water-soluble homopolypeptides (e.g., polylysine·HBr or polyglutamate·Na salt) is sufficient to prevent α -helix formation in aqueous solutions of these samples.⁷ The most studied water-soluble,

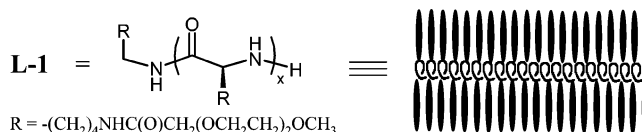


Figure 1. Structure and schematic representation of polymer **L-1**.

nonionic polypeptides, poly(ω -hydroxyalkyl)glutamines (e.g., poly(3-hydroxypropyl)glutamine),⁸ are only weakly α -helical, which is likely a consequence of the low hydrophobicity of the glutamine side-chains. Our solution to this problem was preparation of polypeptides using ethyleneglycol-modified lysine residues.⁹ Short, uniform diethyleneglycol segments provided excellent water solubility, and the increased hydrophobicity of a lysine relative to glutamine backbone resulted in increased helix stability in water. These homopolymers, poly(N_ϵ -2-[2-(2-methoxyethoxy)ethoxy]acetyl-lysine), **1** (Figure 1), were found to be miscible with water in all proportions at ambient temperature, completely α -helical in aqueous solution, and able to form birefringent liquid-crystalline solutions at high weight fractions.⁹ Here, we describe the nature of these aqueous polypeptide liquid crystals in detail.

Results

Optical Observations. Figure 2 shows test tubes filled with increasing volume fractions of polymer **L-1** in water, viewed

[†] University of California, Santa Barbara.

[‡] Université d'Orsay.

- (1) Dujardin, E.; Blaseby, M.; Mann, S. *J. Mater. Chem.* **2003**, *13*, 696–699.
- (2) Thomsen, D. L., III; Keller, P.; Naciri, J.; Pink, R.; Jeon, H.; Shenoy, D.; Ratna, B. R. *Macromolecules* **2001**, *34*, 5868–5875.
- (3) (a) Canet, I.; Meddour, A.; Courtieu, J.; Canet, J. L.; Salaün, J. *J. Am. Chem. Soc.* **1994**, *116*, 2155–2156. (b) Merlet, D.; Ancian, B.; Courtieu, J.; Lesot, P. *J. Am. Chem. Soc.* **1999**, *121*, 5249–5258.
- (4) Hatano, M.; Nozawa, N. *Prog. Polym. Sci. Jpn.* **1972**, *4*, 223–271.
- (5) Block, H. *Poly(γ -benzyl-L-glutamate) and other Glutamic Acid Containing Polymers*; Gordon and Breach: New York, 1983.
- (6) (a) Robinson, C.; Ward, J. C. *Nature* **1957**, *180*, 1183–1184. (b) Robinson, C. *Tetrahedron* **1961**, *13*, 219–234.

- (7) Katchalski, E.; Sela, M. *Adv. Protein Chem.* **1958**, *13*, 243–492.
- (8) (a) Lupu-Lotan, N.; Yaron, A.; Berger, A.; Sela, M. *Biopolymers* **1965**, *3*, 625–655. (b) Lupu-Lotan, N.; Yaron, A.; Berger, A. *Biopolymers* **1966**, *4*, 365–368. (c) Okita, K.; Teramoto, A.; Fujita, H. *Biopolymers* **1970**, *9*, 717–738.
- (9) Yu, M.; Nowak, A. P.; Pochan, D. J.; Deming, T. J. *J. Am. Chem. Soc.* **1999**, *121*, 12210–12211.

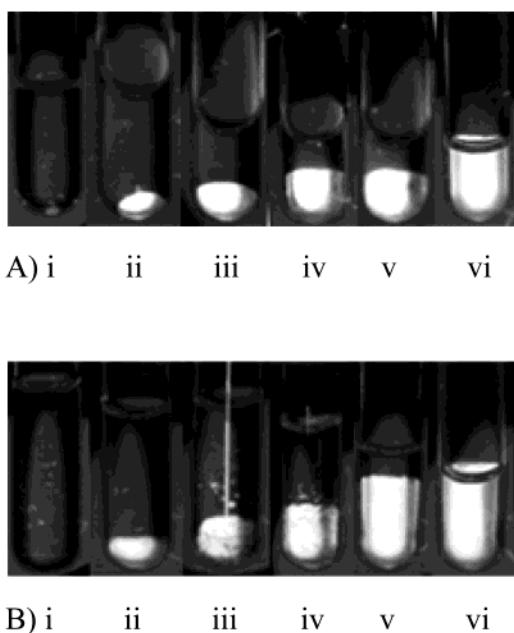


Figure 2. Test tubes filled with increasing weight fractions of **L-1** in deionized water. Samples were imaged between crossed polarizers. (A) ($M_w = 62$ kDa): i = 32.7%; ii = 39.3%; iii = 41.9%; iv = 43.5%; v = 45.4%; vi = 47.9%. (B) ($M_w = 120$ kDa): i = 15.4%; ii = 18.7%; iii = 23.8%; iv = 25.2%; v = 38.5%; vi = 39.8%. All sample compositions are in weight percent.

between crossed polarizers. The upper series contains a low molecular weight sample ($M_w = 62$ kDa), and the lower series contains a high molecular weight sample ($M_w = 120$ kDa); note that the sample concentration ranges differ between the two series. The most dilute samples appear dark because they are isotropic liquids, whereas the most concentrated samples appear bright due to the presence of a liquid-crystalline mesophase. Between these two regimes, a biphasic domain is found where samples display macroscopic phase separation, with the more dense birefringent phase at the bottom of the test tubes. These observations show the existence of a first-order phase transition between the isotropic and liquid-crystalline phases, in addition to confirming that the samples have reached thermodynamic equilibrium. Similar results were also observed for other **L-1** samples with different molecular weights. It should be noted that the liquid-crystalline phase appears at lower volume fractions as the molecular weight of **L-1** increases. The properties of bulk **L-1** samples at elevated temperatures were also investigated; however, no thermotropic behavior was observed. Furthermore, upon heating aqueous **L-1** solutions to ca. 75 °C, the polymers were found to precipitate. This insolubility was presumably due to the loss of H-bonding interactions between the ethylene glycol side-chains and water at elevated temperature.¹⁰

When examined by polarized optical microscopy, the textures of the liquid-crystalline samples held in flat glass capillaries were clear enough to allow mesophase identification. Biphasic samples displayed banded birefringent liquid spherulites floating in a dark isotropic liquid. These spherulites, also called tactoids, are droplets of the anisotropic phase. Fully liquid-crystalline samples displayed large dark homeotropic regions separated by bright regions containing fingerprint patterns (Figure 3). All of

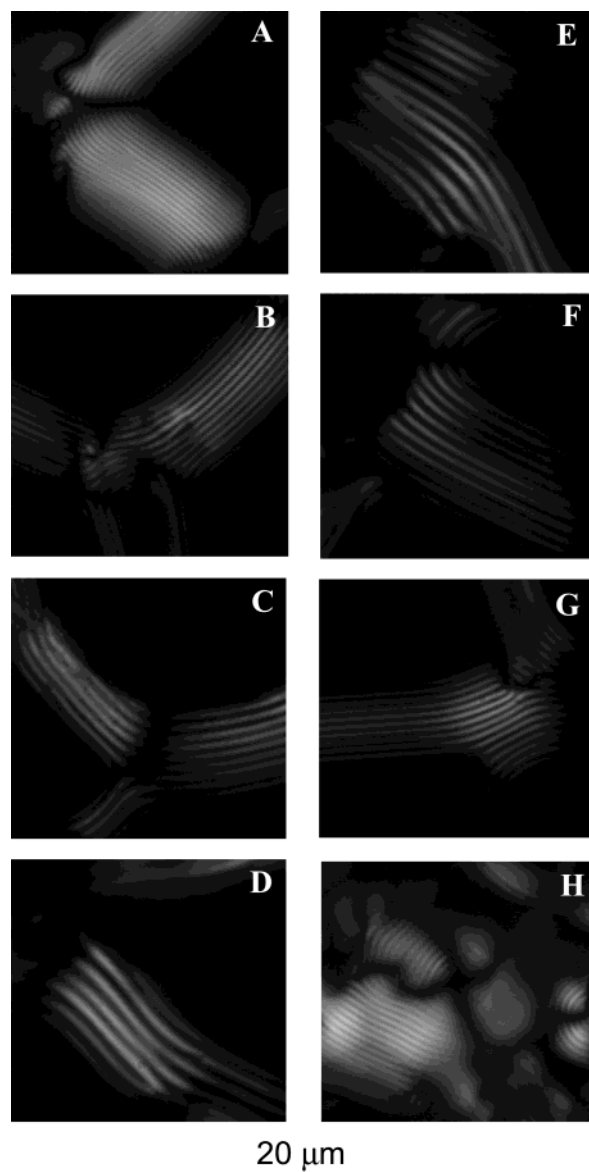


Figure 3. Polarized optical micrographs showing the dependence of the cholesteric pitch on the enantiomeric composition of **1**. All samples were prepared at 60 wt % in deionized water and are defined as the mol % of **L-1** in a **L-1** + **D-1** mixture. (A) = 0%; (B) = 15%; (C) = 30%; (D) = 40%; (E) = 60%; (F) = 70%; (G) = 85%; (H) = 100%.

these features are typical of the cholesteric (i.e., chiral nematic) phase, and the cholesteric pitch could be directly measured from the fingerprint patterns of these micrographs.¹¹

From a practical standpoint, the two major challenges in cholesterics are adjusting and controlling the pitch. As well as being sensitive to solvent and temperature, the pitch also varies with the optical purity of the sample. If a cholesteric liquid-crystalline compound is mixed with its opposite enantiomer (i.e., a mixture of **L-1** and **D-1**), the pitch should increase and approach infinity as the mixture becomes racemic, and then the liquid-crystalline phase will become nematic. To study this point in detail, two polymers of opposite handedness and almost equal molecular weights, **L-1** ($M_w = 59.5$ kDa) and **D-1** ($M_w = 64.9$ kDa), were separately dissolved in deionized water to form 10 wt % solutions. These solutions were then mixed together in

(10) Zalipsky, S.; Lee, C. In *Poly(EthyleneGlycol) Chemistry: Biotechnical and Biomedical Applications*; Harris, J. M., Ed; Plenum: New York, 1992.

(11) de Gennes, P. G.; Prost, J. *The Physics of Liquid Crystals*, 2nd ed.; Clarendon: Oxford, 1993.

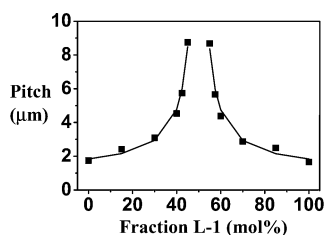


Figure 4. Cholesteric pitch (μm), measured from optical micrographs, as a function of the enantiomeric composition of **1** (mol % of **L-1** in a **L-1** + **D-1** mixture). The solid line is a fit of the data using a hyperbolic divergence at 50 mol %.

the appropriate volumes to give samples with mole fractions of **L-1** from 0% to 100% in 10–15% increments. Circular dichroism spectroscopy was used to verify the degree of enantiomeric mixing in these samples.¹² The sensitivity of the cholesteric pitch to the enantiomeric excess in the samples was observed in optical micrographs (Figure 3). In our samples, the dependence of pitch on mixing ratio was symmetrical around, and increased toward, the 50 mol % mixture (Figure 4). As optical purity increased toward either pure **L-1** or **D-1**, the cholesteric pitch decreased to its minimum value. These data clearly illustrate the fine control of pitch and the cholesteric to nematic transition that can be obtained with the well-defined, rodlike polymer samples utilized here.

Sample Alignment. To gain more information on the structure and stability of these cholesteric phases, we sought to untwist the pitch by aligning the rodlike polypeptide chains. For this purpose, it is well-known that magnetic fields can align α -helical polypeptides parallel to the direction of the applied field.¹³ In preliminary studies, we found that a moderate magnetic field (1.7 T) was not sufficient to align optically pure **L-1** samples, or even the weakest cholesteric samples (i.e., near-equimolar **L-1** + **D-1** mixtures). However, when these weak cholesterics in optical capillaries were placed in a stronger magnetic field (ca. 8 T magnet of an NMR spectrometer), the fingerprint textures were found to disappear as the chains were aligned into a nematic phase. This result showed that strong enough magnetic fields can unwind the cholesteric helical organization in **L-1** + **D-1** mixtures (up to ca. 80 mol % of either **L-1** or **D-1**). Unfortunately, once the samples were removed from the field, the fingerprint textures reappeared in a few minutes as the cholesteric pitch reformed from the untwisted state. Mesophase alignment and relaxation in these samples was readily observed by optical microscopy.¹² In the case of pure **L-1** or **D-1** samples, there appeared to be only partial alignment, which might have been due to the very fast relaxation of these samples during transfer from the magnet to the microscope.

The use of a fast CCD camera and the high beam intensity of a rotating anode X-ray source allowed us to quickly record the scattering pattern of a mixed **L-1** + **D-1** sample (55 mol % **L-1**) that had been aligned in the 8 T magnetic field and then removed for analysis. No sharp diffraction spots or lines were detected, which showed the absence of any positional long-range order (Figure 5). At rest, the scattering patterns were isotropic due to a random orientation distribution of liquid-crystalline domains (Figure 5A). The anisotropic pattern from field alignment showed that the rodlike polypeptides were

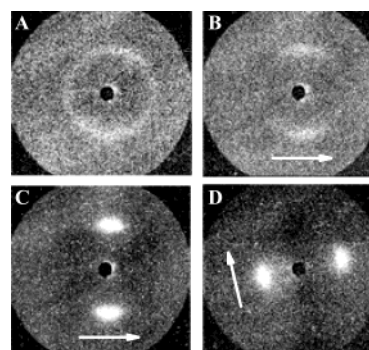


Figure 5. X-ray scattering patterns of liquid-crystalline samples of **1** (60 wt % in deionized water). (A) 100 mol % **L-1** with no applied shear (0 s^{-1}); (B) 100 mol % **L-1** under high shear (400 s^{-1}); (C) 55 mol % **L-1** sample immediately after cessation of applied shear (200 s^{-1} for 10 min); (D) 55 mol % **L-1** sample aligned by magnetic field (8 T) immediately after removal from the field. The arrows indicate the direction of the applied field or shear.

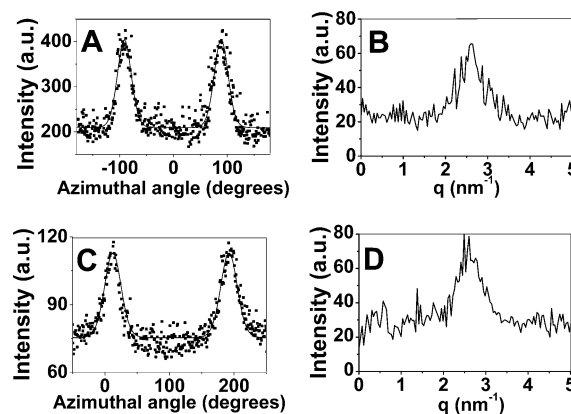


Figure 6. Azimuthal (I versus θ) and radial (I versus q) scans of the X-ray intensity of a 55 mol % **L-1** sample (60 wt % in deionized water) that was either shear aligned (A + B) or magnetic field aligned (C + D). The radial scans each show a broad peak with a maximum at 2.6 nm^{-1} , corresponding to the average distance, 2.4 nm, between the helical rods. The peak width gives an estimate of the correlation length of the liquidlike positional order (ca. 9 nm).

aligned parallel to the magnetic field (Figure 5D), as expected for α -helices.¹³ This is typical of a lyotropic nematic phase comprised of rodlike particles.^{14–17} Thus, the unwinding of the cholesteric twist by the magnetic field, observed by polarized light microscopy, was confirmed to arise from the alignment of the individual helices.

Radial scans (I versus q) of the X-ray intensity scattered in the diffuse spots for the magnetically aligned sample showed a broad peak that had a maximum corresponding to the average distance, 2.4 nm, between the molecular helices. The peak width gave an estimate, 9 nm, of the correlation length of the liquidlike positional order (Figure 6D). Azimuthal scans (I versus θ) of the scattered intensity along a circle going through the maxima of the diffuse spots were used to derive the nematic order parameter S , according to classical procedures (Figure 6C).^{18,19} The value obtained, $S = 0.85 \pm 0.05$, was very large, but is

(12) See Supporting Information.

(13) (a) Panar, M.; Phillips, W. D. *J. Am. Chem. Soc.* **1968**, *90*, 3880–3882. (b) Orwoll, R. D.; Vold, R. L. *J. Am. Chem. Soc.* **1971**, *93*, 5335–5338.

(14) Purdy, K. R.; Dogic, Z.; Fraden, S.; Ruhm, A.; Lurio, L.; Mochrie, S. G. *J. Phys. Rev. E* **2003**, *67*, 031708-1–031708-12.

(15) Oldenbourg, R.; Wen, X.; Meyer, R. B.; Caspar, D. L. D. *Phys. Rev. Lett.* **1988**, *61*, 1851–1854.

(16) Ao, X.; Wen, X.; Meyer, R. B. *Physica A* **1991**, *176*, 63–71.

(17) Keates, P.; Mitchell, G. R.; Peuvrel, E. *Polymer* **1992**, *33*, 3298–3301.

(18) Leadbetter, A. J.; Norris, E. K. *Mol. Phys.* **1979**, *38*, 669–686.

(19) Davidson, P.; Petermann, D.; Levelut, A. M. *J. Phys. II France* **1995**, *5*, 113–131.

typical of lyotropic nematic phases. The X-ray pattern became isotropic in less than an hour as the sample relaxed in the absence of the magnetic field, similar to our optical microscopy observations.

Due to our inability to record structural information in situ during magnetic field alignment, a Couette cell setup was used to shear the liquid-crystalline samples and allow simultaneous recording of their X-ray scattering patterns. Application of a shear flow is a very powerful way of aligning viscous mesophases and has been successfully applied to liquid-crystal phases of PBLG in *m*-cresol.²⁰ For similar alignment of our samples, a small Couette shear cell was built that can be placed in the X-ray apparatus and that requires sample volumes of only ca. 80 μL .¹² The outer cylinder rotates with a controlled angular speed with respect to the fixed inner cylinder. Two classical scattering geometries were used.^{21,22} In the radial configuration, the beam goes through the center of the cell and the velocity/vorticity plane is explored. In the tangential configuration, the X-ray beam is sent through the gap and the velocity gradient/vorticity plane is explored. Comparison of data from these two planes usually allows a full understanding of reciprocal space.

In contrast to the magnetic field studies, all samples that were sheared in the Couette cell did show some degree of alignment. However, the cholesteric phase of the pure enantiomers was found to be too viscoelastic to be completely aligned even at a shear rate of 400 s^{-1} (Figure 5B). Weak cholesterics (**L-1** + **D-1** mixtures) showed the best shear orientation, yet their alignment became markedly more difficult as optical purity was increased. The best alignment was seen immediately after the cessation of shear using a weak cholesteric sample (55 mol % **L-1**) (Figure 5C). The scattering pattern in the radial geometry displayed two symmetrical diffuse spots, whereas the pattern in the tangential geometry showed no anisotropy. The nematic order parameter measured from this scattering pattern ($S = 0.88 \pm 0.05$, Figure 6A,B) is comparable to that measured above using magnetic field alignment. The diffuse spots in Figure 5C represent the intersection with the Ewald sphere of a diffuse torus, perpendicular to the nematic director, due to interparticle interferences. This proves that the rodlike molecules align parallel to the shear flow, as was intuitively expected.

At very high volume fractions of polypeptide (ca. >70 wt %), reached by water evaporation from samples in the unsealed Couette cell, a sharp diffraction line appeared, superimposed over the diffuse spots. This diffraction line was due to the onset of some positional long-range order typical of another mesophase. Its symmetry was determined by recording additional diffraction lines on a different X-ray diffraction setup.¹² Diffraction lines in a ratio 1, $3^{1/2}$, 2, $7^{1/2}$ were observed (Figure 7), which identified the symmetry of this mesophase as hexagonal. This is not surprising because suspensions of rodlike particles often form lyotropic hexagonal mesophases. Upon shearing in the Couette cell, the hexagonal phase became partially aligned as shown by the rather small mosaic spread of the reflection ($\sim 20^\circ$ fwhm). The α -helices, and therefore the C_6 axis, were

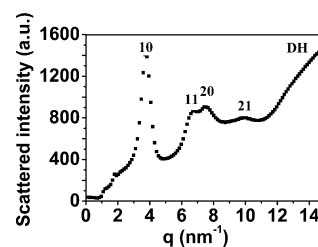


Figure 7. Radial (I versus q) X-ray scattering pattern of a 55 mol % **L-1** sample (>70 wt % in deionized water) showing hexagonal symmetry of mesophase of **1** with diffraction lines in the ratio 1, $3^{1/2}$, 2, $7^{1/2}$ (labeled as the **10**, **11**, **20**, and **21** reflections, respectively). DH = diffuse halo of scattering from ethylene glycol side-chains.

found to orient along the velocity direction like the hexagonal mesophases of other compounds.^{23–26}

Discussion

The phase behavior of concentrated aqueous solutions of **L-1**, **D-1**, and **L-1** + **D-1** mixtures was found to be that predicted by both the Onsager model of the isotropic/nematic phase transition and the numerical simulations on rodlike particles.^{27,28} Qualitatively, the Onsager model and derived theories predict a strongly first-order isotropic/nematic phase transition, with phase coexistence and a large jump of nematic order parameter. These predictions are valid for very long rodlike particles that only interact through purely steric excluded-volume effects. Cholesteric ordering is usually considered as only a small perturbation to the nematic order, so this model should describe the isotropic/cholesteric transition as well. The series of test tubes showing phase coexistence (Figure 2), together with the large value of the nematic order parameter derived from the SAXS patterns, are evidence that the isotropic/cholesteric transition of **L-1**, **D-1**, and **L-1** + **D-1** mixtures can be explained by the Onsager model. Moreover, we believe that electrostatic interactions are negligible in this system because similar properties were observed when samples were prepared in NaCl solutions (100 mM) where any electrostatic interactions were screened. An additional prediction of the Onsager model is that temperature should have no influence on the phase transition. However, this prediction could not be tested here because all liquid-crystalline samples became turbid upon heating. This observation is likely related to the complex miscibility of PEG with water as a function of temperature.¹⁰

To analyze this system more quantitatively, the Onsager model predicts the volume fractions Φ_n and Φ_i of the nematic and isotropic phases at the transition: $\Phi_n = 4.2$ D/L and $\Phi_i = 3.3$ D/L. For a short **L-1** ($M_w = 62$ kDa; $L = 32.3$ nm and $D = 2.2$ nm), we obtained $\Phi_n = 29\%$ and $\Phi_i = 23\%$. These results are in fair agreement with the experimental values of 47% and 38%, respectively, all the more because the Onsager model only gives quantitative predictions for very long rods ($L/D > 100$). It is also likely that the experimental values are higher than predicted because the α -helix does have some finite flexibility,

(23) Imp rator-Clerc, M.; Davidson, P. *Eur. Phys. J. B* **1999**, *9*, 93–104.

(24) Ramos, L.; Molino, F.; Porte, G. *Langmuir* **2000**, *16*, 5846–5848.

(25) Hamley, I. W. *The Physics of Block-Copolymers*; Oxford University Press: New York, 1998.

(26) Camerel, F.; Gabriel, J. C. G.; Batail, P.; Davidson, P.; Lemaire, B. J.; Schmutz, M.; Gulik-Krzywicki, T.; Bourgaux, C. *Nano Lett.* **2002**, *2*, 403–407.

(27) Onsager, L. *Ann. N.Y. Acad. Sci.* **1949**, *51*, 627–659.

(28) Vroege, G. J.; Lekkerkerker, H. N. W. *Rep. Prog. Phys.* **1992**, *55*, 1241–1309.

(20) Ugaz, V. M.; Cinader, D. K., Jr.; Burghardt, W. R. *J. Rheol.* **1997**, *42*, 379–394.

(21) Molino, F. R.; Berret, J. F.; Porte, G.; Diat, O.; Lindner, P. *Eur. Phys. J. B* **1998**, *3*, 59–72.

(22) Hamley, I. W.; Pople, J. A.; Fairclough, J. P. A.; Terrilli, N. J.; Ryan, A. J.; Booth, C.; Yu, G. E.; Diat, O.; Almdal, K.; Mortensen, K.; Vilgud, M. *J. Chem. Phys.* **1998**, *108*, 6929–6936.

especially with the poly(lysine) backbone, which may serve to effectively decrease L .²⁹ For a longer **L-1** ($M_w = 120$ kDa; $L = 62.6$ nm and $D = 2.2$ nm), the predicted volume fractions were $\Phi_n = 15\%$ and $\Phi_i = 12\%$, as compared to the experimental values of 39% and 17%, respectively. Here, the experimental biphasic gap (Φ_n/Φ_i) was much larger than the prediction, which could be due to sample polydispersity.²⁸ Altogether, these theoretical considerations suggest that the α -helical polypeptides **D-1** and **L-1** are essentially rodlike and that their interactions in water are purely steric.

The formation of a chiral nematic phase in concentrated solutions is a predictable outcome for these polypeptides. A typical average distance d between rods was obtained from the positions of the maxima of the diffuse scattering spots. Assuming a local hexagonal packing of rods, this distance is related to the sample volume fraction ϕ by the formula $d = 1.65\phi^{-1/2}R$, where R is the apparent rod radius. This gives us $R = 1.1$ nm in good agreement with estimations from molecular modeling (1.21 nm). The formation of a hexagonal columnar mesophase at volume fractions above that of the cholesteric phase is also expected for rods that are monodisperse in diameter. From our results, it appears that the phase diagram of **D-1** and **L-1** in aqueous solution is similar to that of PBLG in organic solvents.²⁰

However, the aqueous system of **D-1** and **L-1** does show some notable differences from organic systems employing PBLG. At comparable chain lengths, PBLG forms the liquid-

crystalline phase at significantly lower volume fractions. This phenomenon might be due to the increased flexibility of the α -helix with a lysine backbone as compared to glutamate, as mentioned above. It might also be related to differences in the polymer-solvent interactions, which are likely greater for **1** in water than those for PBLG in organic solvents. The solvent interactions for **1** are stronger because the ethylene glycol side-chains are solubilized by H-bonding to water, leading to weaker interactions between the polypeptide chains and the need for higher volume fractions to induce ordering. Aside from these differences, the cholesteric phase of **1** can be well understood by analogy to the PBLG system. As such, our results show that there is now a simple homopolypeptide system that provides robust, water-based cholesteric liquid crystals with predictable properties. This system may find use in biomimetic composite materials synthesis, characterization of optically active compounds as an NMR solvent, and for performing asymmetric catalysis in an aqueous environment.

Acknowledgment. We are deeply indebted to D. Dallé and B. Kasmí for the design of the Couette shear cell apparatus. This work was supported by the National Science Foundation MRSEC Program DMR-0080034. E.G.B. thanks the UCSB MRL for an Executive Vice Chancellor's Travel Fellowship.

Supporting Information Available: Details of all materials and measurements. This material is available free of charge via the Internet at <http://pubs.acs.org>.

JA047932D

(29) Daniel, E.; Katchalski, E. In *Polyamino Acids, Polypeptides, and Proteins*; Stahmann, M. A., Ed.; University of Wisconsin Press: Madison, WI, 1962; p 183.